

# Electric Field Distribution in a Biological Cell for Various Electrode Configurations-A Simulation Study

Md. Osman Goni

Department of Electronics and Communication Engineering  
Khulna University of Engineering & Technology  
osman\_goni@yahoo.com

**Abstract**— Electroporation or electro-permeabilization (EP) is a non-viral physical process of inducing and/or increasing permeability of biological membranes by the application of high intensity and short duration electrical pulses. The resulting high field strength in the membrane can lead to the formation of regions of increased permeability, often called pores that allow transmembrane transport of macromolecules, such as DNA and chemo drugs. The efficacy of EP depends on a number of parameters, such as electric field strength, duration, number of pulses, size of target cell, and type of drug or DNA to be fed, to mention a few parameters. While electric field strength, duration, and number of pulses are the dominant parameters for the electroporation effect, the electric field distribution also depends on the shape, the size, and the material of electrodes used. The various electrodes used in practice are the parallel plate electrodes, the needle electrodes, the needle array electrodes, and the caliper electrodes. Both six needle array and parallel plate electrodes were used in the skin cancer trials. The electric field distribution varies with the type of electrode. The choice of electrodes depends upon the type of application. For example, parallel plate electrodes produce good results in human clinical trials and the distance between the electrodes can be easily varied. Needle electrodes are the simplest, but due to their configuration, the field distribution is highly nonlinear; there is higher field strength around the needle tip. That is one of the reasons for using multiple needles or needle arrays to make the field distribution as uniform as possible. It is of practical interest to study the electric field distribution of various electrodes to make a more informed choice of which electrodes to use. This

paper presents the results of a study of the electric field distribution in biological tissues for various electrode configurations. Magwel was used in this study. For the same voltage applied, the triangular and arc electrode configuration developed the highest electric field strength. Specifically, we develop simulation results that enhance or enable the acquisition of information from cells.

**Index Terms**— Cell culture, dielectrophoresis, electrodes, HeLa cell.

## I. INTRODUCTION

Electroporation is the physical process of inducing transient permeability of biological membranes by short pulses of electric fields [1-3]. The resulting high field strength in the membrane can lead to the formation of areas of increased permeability, often called pores, which allow transmembrane transport of molecules. This effect has been used in the laboratory for more than a decade as a research tool to facilitate cellular uptake of genetic material in vitro. More recently, electroporation has also been found effective for the intracellular delivery of molecules in living tissues, which led to a variety of medical applications. Some of these applications have already proceeded to clinical trials. The effectiveness of this technique is evidenced by the Phase I and II skin cancer clinical trials [3]. The most important parameters for effective electroporation are the electrical field strength and the length of time the field applied (pulse length) [4, 5]. A number of other parameters can affect the efficacy of electroporation, such as the shape of the electrical pulse, polarity, number of and interval between pulses, size of target cells, and thermal conditions during and after the pulse, as

well as other cellular and environmental factors [4-7]. Electric field in the tissue is generated by a potential difference (voltage) between electrodes surrounding, or adjacent to, the tissue. A wide variety of electrode configurations have been developed, appropriate for each specific therapeutic goal [8, 9].

## II. NEED FOR DIFFERENT CONFIGURATIONS OF ELECTRODES

The role of the electrodes is to act as a conduit to transform the voltage pulse from a pulse generator into local electric fields in tissues. The most commonly used electrodes are parallel plate electrodes [3, 8, and 9] and needle electrodes—either a six needle array [3, 8-10] or two needles [11] are used [12].

(a) Parallel plate electrodes. It's the simplest configuration and it produces good results in human clinical trials with tumors close to the surface due to the uniform electric field it develops [8]. With parallel plate electrodes, it is very easy to adjust the distance between them to obtain the desired field strength. However, plate electrodes are less efficacious for deeper tumors, where needle electrodes are more useful [8].

(b) Needle Electrodes. A pair of needles is also a very simple system [8, 11]. However, due to the needle configuration, the field of single-pair-needle electrodes is highly divergent, with high field strength near the needle tip. That is one of the reasons why multiple needles or needle arrays are needed to develop a more even electric field distribution [8]. Apparently, different cross sections of the electrodes will affect the electric field distribution. In this paper, the electric field distributions due to various electrode configurations are studied using Magwel [13].

## III. ELECTRODES

To manipulate cells, one must create an electric field of a certain shape and strength. The two approaches to doing this are to either integrate electrodes within the microsystem or have them be external [14].

### A. Internal electrodes

Internal electrodes, uncommon in EP systems, are the predominant approach to generating electric fields for dielectrophoresis (DEP), mainly

because of the superior control they offer for locally shaping the field. Electrodes act as equipotential surfaces that shape the field by controlling their location and voltage. Above, we saw that reducing the length of the electrodes favorably affected manipulation forces, and the simplest way to do this is to place electrodes close together. This necessitates electrodes that are internal to the system. The primary consideration that arises when using internal electrodes is that the electrodes can adversely interact with the electrolyte via either gas generation or corrosion. Because current is carried in metals by electrons and in electrolytes by ions, electrochemistry must occur at the electrode-electrolyte interface to transform the electron current into an ion current. The net result can be the production of gas ( $H_2$ ,  $O_2$ , etc.) or dissolution of the electrode, both of which can disrupt operation of the device. This is a serious concern at dc, explaining the relative absence of EP systems that use internal electrodes. For DEP systems, electrochemical effects are typically avoided by operating at  $>10$ 's kHz in saline (lower frequencies can be tolerated in liquids of lower ionic strength). Gas generation is also voltage dependent, so higher voltages are more likely to lead to deleterious effects. Given that one usually wishes to operate at a high frequency ( $>100$ 's kHz) when using DEP with cells, electrochemistry does not pose any practical limitations.

### B. External electrodes

The alternate approach is to use external electrodes. Very common in EP systems, external electrodes are rare in DEP systems. One advantage of using external electrodes is that they do not have to be fabricated with the device, resulting in a simpler fabrication process. The electrodes themselves often consist of platinum wires that are inserted into the port holes of the device. The electric field in systems that use external electrodes is shaped by using a straight channel (for EP) or inserting low polarizability obstructions (such as glass or polymer posts [15, 16]) in the channel (for DEP). There is no theoretical limit to the electric fields and forces that can be generated using external electrodes, although there are practical limits. Higher overall fields (such as for EP) are created by increasing the voltage or decreasing the spacing between the

obstructions, limited by the fact that openings cannot be made any smaller than the cells. Additionally, the fields exist throughout the volume of the electrolyte, which can lead to significant heating. Thus, published DEP devices for use with cells have typically used very-low conductivity water to minimize heating [15, 16]. Finally, fairly large voltages (approx. 0.1~1 kV) are needed to generate the required fields, and thus, these devices are limited to dc or low-frequency operation. This is fine for EP, which operates at dc, but restricts DEP manipulations to only the low frequency region of the Clausius-Mossotti (CM) factor. The need to minimize solution conductivity, operate at or near dc, and minimize chamber volume make external electrodes best suited for use with robust cells—such as bacteria—that can tolerate being placed in low-conductivity buffers or as endpoint analysis on cells that are not needed for downstream use.

### C. Effects of electric field on cell

Because electrical cell manipulation exposes cells to strong electric fields, one needs to know how these electric fields might affect cell physiology. Ideally, one would like to determine operating conditions that will not affect the cells and use those conditions to constrain the design. Of course, cells are poorly understood complex systems and thus it is impossible to know for certain that one is not perturbing the cell. However, all biological manipulations—cell culture, microscopy, flow cytometry, etc.—alter cell physiology. What is most important is to minimize known influences on cell phenotype and then use controls to account for unknown influences. The known influences of electric fields on cells can be split into the effects due to current flow, which causes heating, and direct interactions of the fields with the cell. We consider each of these in turn.

## IV. SIMULATION MODEL

We chose the multiphysics model (conductive and dielectric media dc & electrostatics model) when using Magwel. The general model cell culture system with the HeLa cell is shown in Fig. 1. Tables 1 and 2 give the dimensions and other electrical data used in this simulation, respectively.

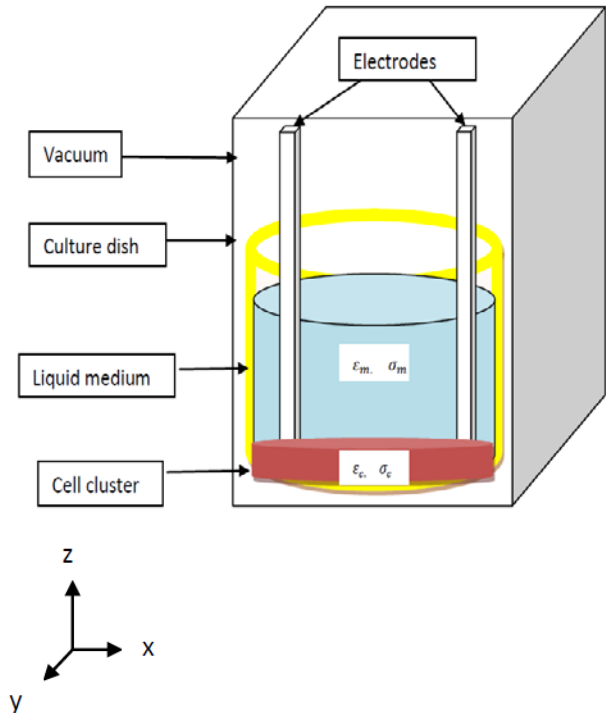


Fig. 1. 3D view of the simulation domain for the cell culture system.

Modeling of cell and medium: Figure 1 shows the schematic view of the cell culture system in which the HeLa cell is considered as a monolayer of cells located at the bottom of the culture dish. The cell is modeled as a homogeneous sphere with a diameter of 35  $\mu\text{m}$  and a thickness of 3  $\mu\text{m}$ . On the other hand, the culture medium is modeled as DMEM with 5 mm of height. Both the cell and the medium have their corresponding electrical parameters at different frequencies as listed in Table 1. The copper electrodes are used to apply electric field into the culture dish and are modeled as internal electrodes. The dimension and shape of the electrodes influence the generation of the E field in the vicinity of the electrodes which in turn induces field in the cell.

Table 1: Simulation parameters

Simulation domain	50 mm X 50 mm X 15 mm
Culture dish	circular type flux, diameter= 35 mm, height= 9.5 mm
Cell culture medium	Dulbecco's Modified Eagle Medium (DMEM), height=5mm
Cell	Circular, monolayer, diameter= 35 mm, height= 3 $\mu$ m
Electrodes (internal)	Copper, height=15mm (with different shape)
Spacing between electrodes	1mm
Applied voltage	10 V at f= 100 kHz (small signal)

Table 2: Dielectric properties of the HeLa cell and culture medium [17, 18]

Frequency	Cell E	Cell $\sigma$	Medium $\epsilon$	Medium $\sigma$
1Hz	6.0e4	0.0001	80	1.6
100Hz	5.5e4	0.0007	78	1.55
100kHz	5 e4	0.001	76	1.5
1MHz	1.5e4	0.06	74	1.5

### A. Angular plate electrodes configuration

The copper electrodes are placed inclined (V-shaped) in the layer of cell and medium as shown in Fig. 2(a). The contact is facilitating the input bias to the electrodes. Here the left electrode has a 10 V dc while the right one is at ground state (0 V). A small signal is also considered to the analysis with ac with frequency of 100 kHz. The small gap (1 mm) is maintained between the lower parts making angular orientation. Figures 2(b), 2(c), and 2(d) show the results with potential distribution, E field distribution, and magnetic vector potential, respectively. The higher electric

field intensity region is clearly observed at the smallest gap between the electrodes.

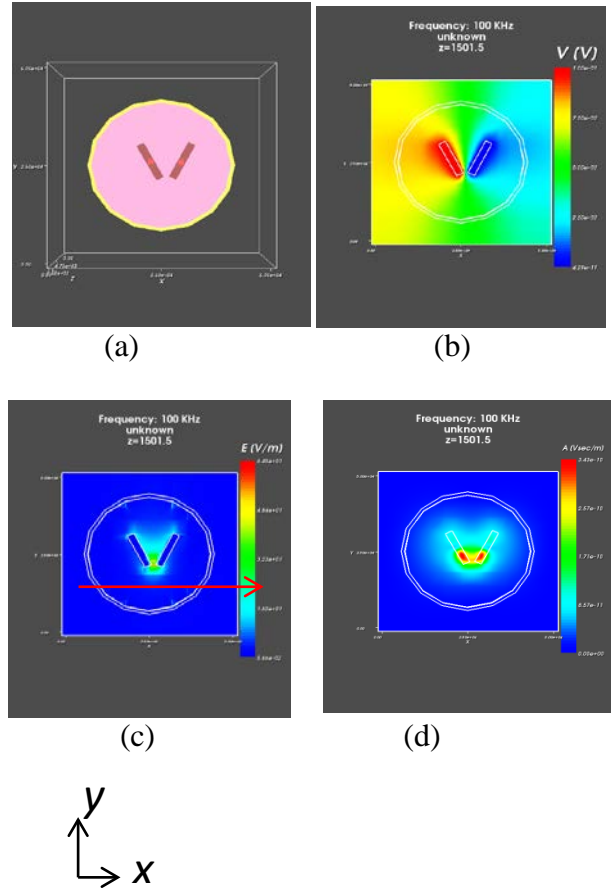


Fig. 2. Simulation model for the HeLa cell using inclined electrodes (x-y plane, at  $y=21553 \mu\text{m}$  and  $z=1501 \mu\text{m}$ , at the position of cell layer marked with red arrow) (a) Cell layer view, (b) potential distribution, (c) spatial E field distribution, and (d) magnetic vector potential.

We have plotted the E field intensity in the x direction at  $y=21553 \mu\text{m}$  and  $z=1501 \mu\text{m}$  (cell layer) as shown in Fig. 3. The sharp peak electric field strength at the gap of the electrodes is 64.5 V/m which is the actual field strength obtained in the center of the electrodes. The nominal field strength (voltage divided by the distance between the two electrodes) is 10 kV/m.

So, we can tell the actual field strength is much lower than the nominal value. This is true because field will be reduced inside the dielectric bodies as the cell having greater value of permittivity than the outside liquid medium. Two

other minor peaks are also observed at the both side of the main peak. Those are the interfacial field due to the conductor-dielectric interface.

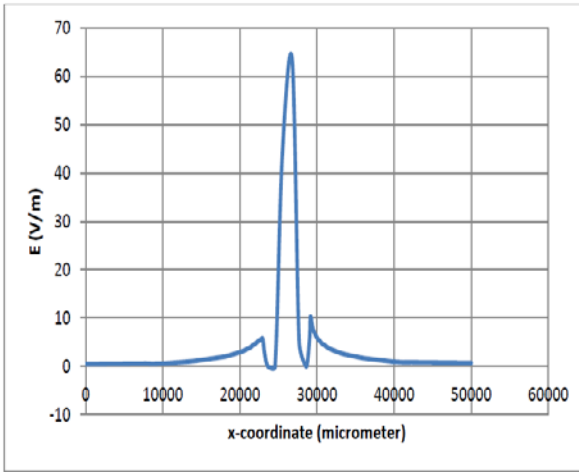


Fig. 3. E field variation along x axis at  $y=21553 \mu\text{m}$  and  $z=1501 \mu\text{m}$  at  $f=100 \text{ kHz}$ .  $E_{\text{max}}=64.5 \text{ V/m}$  using inclined electrodes as shown in model of Fig 2(a).

**B. Triangular electrodes configuration**

This model is simulated using two triangular shape electrodes placed at the same gap in between the electrodes. The results of E field distribution are plotted with the function of x-coordinates (micrometer). Figure 5 shows the E field variation along the x axis at  $y=26608 \mu\text{m}$  and  $z=1501 \mu\text{m}$  at  $f=100 \text{ kHz}$ . The maximum electric field is found to be  $105 \text{ V/m}$  right at the gap of the electrodes. The sharp and pointed peak is found due to the symmetry in the discretization of electrodes.

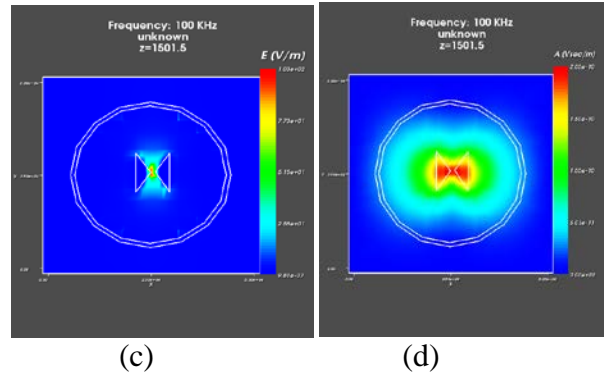
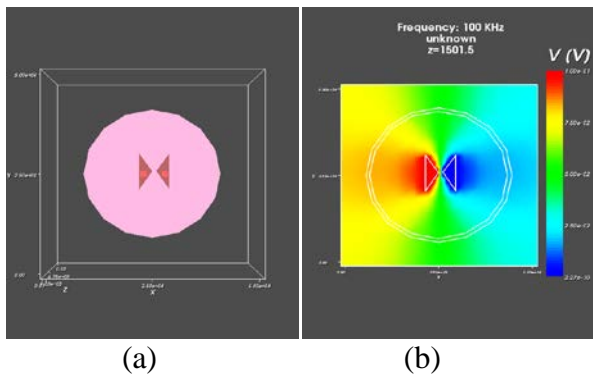


Fig. 4. Simulation model for the HeLa cell using triangular electrodes (a) cell layer view, (b) potential distribution, (c) spatial E field distribution, and (d) magnetic vector potential.

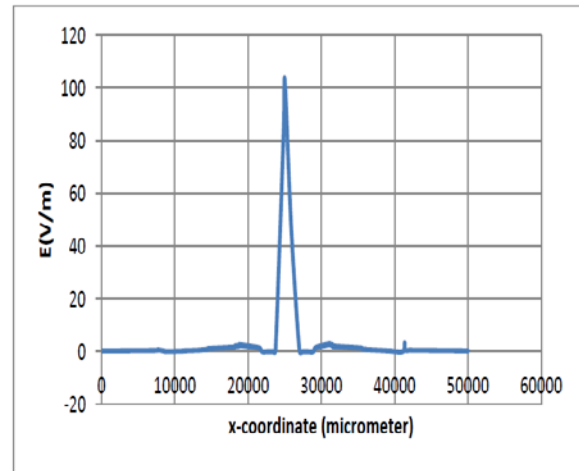


Fig. 5. E field variation along x axis at  $y=26608 \mu\text{m}$  and  $z=1501 \mu\text{m}$  at  $f=100 \text{ kHz}$ .  $E_{\text{max}}=105 \text{ V/m}$  using inclined electrodes as shown in the model of Fig 4(a).

**C. Needle electrodes configuration**

The electric field distribution is not smooth near to the gap of electrodes as in Fig 6(a). Because the field is highly non-uniform due to the geometry of electrodes and no linear discretization effect at the electrodes edges that can be seen from Figs. 6(b), 6(c), and 6(d).

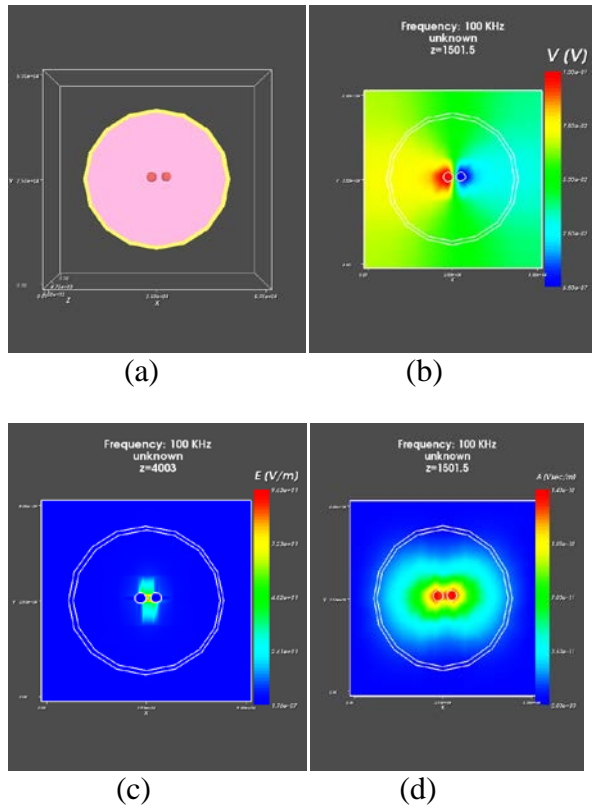


Fig. 6. Simulation model for the HeLa cell using needle electrodes (a) cell layer view, (b) potential distribution, (c) spatial E field distribution, and (d) magnetic vector potential.

Figure 7 shows the variation of E field along the x axis at  $y=26045 \mu\text{m}$  and  $z=1501 \mu\text{m}$  (cell layer) at  $f=100 \text{ kHz}$ . The maximum E field is observed to be  $96 \text{ V/m}$ . The neighboring effect of the conductive electrodes and conductor-dielectric interface would produce such an effect which can be noticed from a small rise-up at both sides of the main peak.

**D. Parallel plate electrodes configuration**

In this configuration model shown in Fig. 8(a) and the simulation results Figs 8(b), 8(c) and 8(d), the electric field distribution is found quite smooth and comparatively even at the entire gap of electrodes. Because the field is uniform due to the geometry of electrodes and also linear discretization is possible at the electrode edges. The high level electric field strength occurs between the cell and electrodes plates. Figure 9 shows the variation of E field along x axis at  $y=20400 \mu\text{m}$  and  $z=1503 \mu\text{m}$  (cell layer) at  $f=100 \text{ kHz}$ . The maximum E field is observed to

be  $96 \text{ V/m}$ . The neighboring effect of the conductive electrodes and conductor-dielectric interface produce small rise-up at the both side of the main peak.

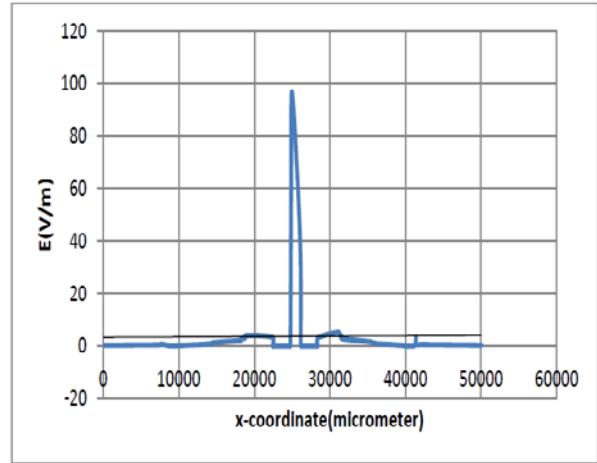


Fig. 7. E field variation along x axis at  $y=26045 \mu\text{m}$  and  $z=1501 \mu\text{m}$  at  $f=100 \text{ kHz}$ .  $E_{\text{max}}=96 \text{ V/m}$  using needle electrodes as shown in model of Fig. 6(a).

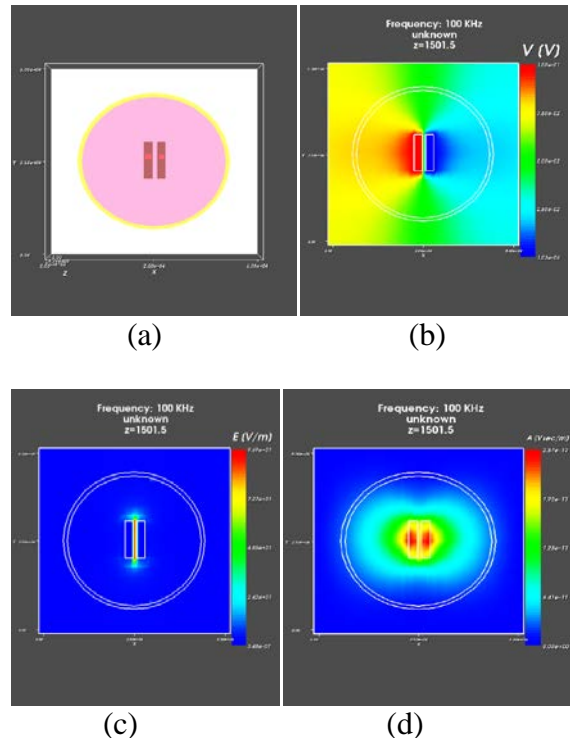


Fig. 8. Simulation model for the HeLa cell using parallel electrodes (a) Cell layer view, (b) potential distribution, (c) spatial E field distribution, and (d) magnetic vector potential.

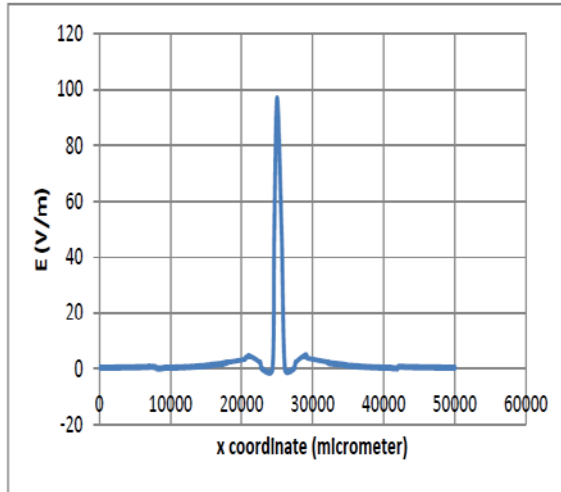


Fig. 9. E field variation along x axis at  $y = 20400 \mu\text{m}$  and  $z = 1503 \mu\text{m}$  at  $f = 100 \text{ kHz}$ .  $E_{\text{max}} = 96 \text{ V/m}$  using parallel electrodes as shown in model of Fig 8(a).

### E. Arc electrodes configuration

The non-smooth electric field distribution is found at the entire gap of electrodes shown in model and their results in Figs. 10(a) and 10(b). Because the field is non-uniform due to the geometry of electrodes and linear discretization is difficult to achieve at the electrodes edges. Figure 11 shows the variation of E field along x axis at  $y = 26181 \mu\text{m}$  and  $z = 1501 \mu\text{m}$  (cell layer) at  $f = 100 \text{ kHz}$ . The maximum E field is observed to be  $134 \text{ V/m}$ .

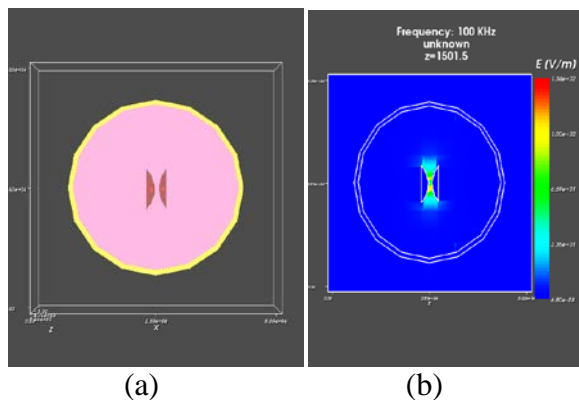


Fig. 10. Simulation model for the HeLa cell using inclined electrodes (a) cell layer view, (b) spatial E field distribution.

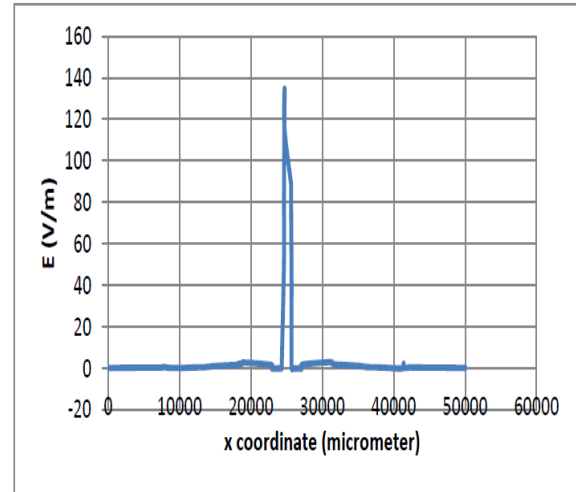


Fig. 11. E field variation along x axis at  $y = 26181 \mu\text{m}$  and  $z = 1501 \mu\text{m}$  at  $f = 100 \text{ kHz}$ .  $E_{\text{max}} = 134 \text{ V/m}$ .

Table 3 summarizes the results of the simulation of the HeLa cell model using different type and shape of the electrodes. The shape of the electrodes characterizes the linearity of the field distribution at the edges. The highest electric field strength due to highly non-uniformity occurs at the area closest to the sharp point. Domain discretization at the structure of interest is also important for the accurate results. The peak electric field exists only at the spacing (gap) of the electrodes. Hence, the location, shape, and orientation of the electrodes influence the overall contribution of the E field to the cell and medium. For the monolayer of the HeLa cell, the localized electric field as obtained from the above field distribution does not affect the entire layer of the cell. Thus, the average electric field should be more pronounced and effective for the polarization of the dielectric properties of the cell. In that case, the array of electrode could be a good choice where the uniform distribution is important. For the manipulation of small dielectric objects (cell), different types of array like interdigitated or polynomial electrodes array can also perform better than single electrode.

Table 3: Comparison of E fields with electrode's type and their orientations

Electrode's types and orientation	Maximum E field (V/m)	Uniformity
Flat and angular	64.5	Non uniform
Triangular	105	Non uniform
Rod (pin)	96	Non uniform
Flat and parallel	96	Uniform
Arc	134	Non uniform

## V. CONCLUSION

The simulation of a monolayer of HeLa cell is presented here with the different types, shape, and orientation of electrodes. The electric field distribution for electroporation applications strongly depends on the electrode configurations. Parallel plate electrodes and needle electrodes of various dimensions are most commonly used for preclinical and clinical applications [3, 8-10]. Parallel plate electrodes give the most uniform electric field distribution with the simplest configuration as seen in this simulation and this correlates well with the published data [8]. Needle electrodes need to be used for deeply-seated tumors where parallel plate electrodes cannot be used. Due to the sharp needle point, needle electrodes give non-uniform field distribution with the highest field strength near the tip of the needle as the field homogeneity depends on the shape of the electrodes [19-21]. This point has to be taken into consideration during electroporation applications since the electric field in the tissue will be different for a given area and hence the efficacy of the technique will vary.

The cell and the medium are equivalently characterized by their electrical constants at certain frequency. As the medium is considered to be dispersive, the results are shown to be at certain frequency namely 100 kHz. It was found that up to 100 MHz, the results does not differ significantly as the size of the cell is much less than the wavelength (low frequency problem). The work also demonstrates the proper choice of the electrodes would be significant for the cell manipulation and cell culture.

The presented ideas facilitate the dielectrophoresis as a building block for lab-on-a-chip devices which can be easily fabricated using the existing microelectrode photolithography techniques. The design of the electrodes, the choice of the suspending medium, the applied peak voltage and frequency can be pre-determined to optimize the operation of the device.

## REFERENCES

- [1] L. M. Mir, et al., Electrochemotherapy, "A Novel Antitumor Treatment: First Clinical Trial C. R.," *Acad. Sci.*, Paris 313, pp. 613-618, 1991.
- [2] R. H. Heller, "Overview of Electroporation," *Technology in Cancer Research & Treatment*, vol. 1, no. 5, 2002.
- [3] R. Heller, R. Gilbert, and M. J. Jaroszeski, "Clinical Trials for Solid Tumors using Electrochemotherapy," in *Electrochemotherapy, Electrogenotherapy, and Transdermal Delivery*, New Jersey: Humana Press, pp. 137-156, 2000.
- [4] M. P. Rols, et al., "In Vivo Delivery of Drugs and Other Molecules to Cell," in *Electrochemotherapy, Electrogenotherapy, and Transdermal Delivery*, New Jersey: Humana Press, pp. 83-97, 2000.
- [5] L. M. Mir and S. Orlowski, "The Basis of Electrochemotherapy," in *Electrochemotherapy, Electrogenotherapy, and Transdermal Delivery*, Humana Press, pp. 99-117, 2000.
- [6] H. Potter, "Molecular Genetic Applications of Electroporation," in *Electroporation and Electrofusion in Cell Biology*. New York: Plenum Press, pp. 319-341, 1989.
- [7] T. Curd, B. Vernon, C. Pauken, and R. Sundararajan, "Optimization of Electroporation Parameters for Human Ovarian Cancer Cells", *Proceedings of Electrostatics Society of America (ESA) Annual Meet*, University of Alberta, Edmonton, Canada 2005.
- [8] G. A. Hofmann, "Instrumentation and Electrodes for In Vivo Electroporation", in *Electrochemotherapy, Electrogenotherapy, and Transdermal Delivery*, New Jersey: Humana Press, pp. 37-61, 2000.
- [9] R. Gilbert, M. Jaroszeski, and R. Heller, "Novel Electrode Designs for Electrochemotherapy", *Biochimica et Biophysica Acta*, vol. 1334, pp. 9-14, 1997.
- [10] T. Goto et al., "Combination Electro-Gene Therapy Using Herpes Virus Thymidine Kinase and Interleukin-12 Expression Plasmids is Highly Efficient Against Murine Carcinomas In Vivo". *Mol. Therapy*, vol. 10, no. 5, p. 929-937 (2004).
- [11] Y. Yamashita et al., "Electroporation-Mediated Interleukin-12 Gene Therapy for Hepatocellular



- Carcinoma in the Mice Model”, *Cancer Res.*, vol. 61, pp. 1005-1012, 2001.
- [12] W. Mitchell and R. Sundararajan, “Electric Field Distribution in Biological Tissues for Various Electrode Configurations-A FEMLAB Study”, *Proc. of the COMSOL Multiphysics User’s Conf.*, Boston, 2005.
- [13] Magwel, SolvEM User Guide, Version 3.0.0, ©Magwel, <http://www.magwel.com/> Sep 2008.
- [14] Joel Voldman, “Electrical Forces for Microscale Cell Manipulation”, *Annu. Rev. Biomed. Eng.* 8: pp. 425-54, 2006.
- [15] C. F. Chou, J. O. Tegenfeldt, O. Bakajin, S. S. Chan, E. C. Cox, et al. “Electrodeless Dielectrophoresis of Single- and Double-Stranded DNA”, *Biophys. J.*, vol. 83, pp. 2170-79, 2002.
- [16] B. H. Lapizco-Encinas, B. A. Simmons, E. B. Cummings, Y. Fintschenko, “Dielectrophoretic Concentration and Separation of Live and Dead Bacteria in an Array of Insulators”, *Anal. Chem.* vol. 76, pp. 1571-79, 2004.
- [17] M. H. Wang, M. K. Chen, and L. S. Jang, “Electrical Characterization of Single HeLa Cell using 2D Simulation and Spectroscopy Measurement”, *IEEE proceedings*, CIBEC 2008.
- [18] Y. Nikawa and T. Michiyama, “Blood-Sugar Monitoring by Reflection of Millimeter Wave”, *Proceedings of Asia-Pacific Microwave Conf.* 2007.
- [19] J. Suehiro, G. B. Zhou, M. Imamura, and M. Hara, “Dielectrophoretic Filter for Separation and Recovery of Biological Cells in Water”, *IEEE Trans. Indus. Appl.*, vol. 39, pp. 1514-21, 2003.
- [20] Z. Z. Cvetkovic, B. Petkovic, M. Peric, “Systems for Homogeneous Electric Fields Generation and Effects of External Bodies on Field Homogeneity,” *Applied Computational Electromagnetic Society (ACES) Journal*, vol. 26, no. 1, pp. 56-63, Jan. 2011.
- [21] D. M. Velickovic and Z. Z. Cvetkovic, “Homogeneous Electric Field Generation using Biconical Electrodes”, *Proceedings 21<sup>st</sup> Int’l Conf. on Microelectronics*, vol. 1, pp. 209-212, Sep. 14-17, 1997.